Title: Tracer experiment using 42K+ and 137Cs+ revealed the different transport rates of potassium and caesium within rice roots

Author: Natsuko I. Kobayashi, Ryohei Sugita, Tatsuya Nobori, Keitaro Tanoi and Tomoko M. Nakanishi

Kobayashi Natsuko I., Sugita Ryohei, Nobori Tatsuya, Tanoi Keitaro, Nakanishi Tomoko M. (2016) Tracer experiment using $^{42}K^{+}$ and $^{137}Cs^{+}$ revealed the different transport rates of potassium and caesium within rice roots. *Functional Plant Biology* **43**, 151–160.

DOI: 10.1071/FP15245

Title

Tracer experiment using $^{42}K^+$ and $^{137}Cs^+$ revealed the different transport rates of potassium and cesium within rice roots

Abridged title

Tracer study to differentiate between Cs^+ and K^+ transport

Authors

Natsuko I. Kobayashi[A], Ryohei Sugita[A], Tatsuya Nobori[A, B], Keitaro Tanoi[A] and Tomoko M. Nakanishi[A]

Affiliation and address

[A]Graduate School of Agricultural and Life Sciences, The University of Tokyo 1–1–1 Yayoi, Bunkyo-ku, Tokyo 113–8657, Japan

[B] Department of Plant Microbe Interactions, Max Planck Institute for Plant Breeding Research, Cologne, Germany

Kobayashi, NI; anikoba@mail.ecc.u-tokyo.ac.jp

Sugita, R; ryo818@hotmail.co.jp

Nobori, T; tatsuyanobori@gmail.com

Tanoi, K; uktanoi@mail.ecc.u-tokyo.ac.jp

Nakanishi, TM; atomoko@mail.ecc.u-tokyo.ac.jp

Corresponding Author

Keitaro Tanoi

uktanoi@mail.ecc.u-tokyo.ac.jp

Tel: +81 3 5841 5440

Fax: +81 3 5841 8193

Number of tables and figures

Tables 2

Figures 4

Abstract

The differences in the transport characteristics *in planta* between potassium (K^+) and cesium (Cs^+) was investigated using their radionuclides, $^{42}K^+$ and $^{137}Cs^+$. A tracer experiment using nutrient solutions supplemented with ^{42}K and ^{137}Cs revealed that the ratio of the root's K^+ uptake rate to its Cs^+ uptake rate was 7 to 11 times higher than the K^+/Cs^+ concentration ratio in the solution, and the number was varied depending on the K concentration in the solution and also on the growth condition. After entering through the root tissues, the $^{42}K^+/^{137}Cs^+$ ratio in the shoots was 4.28 times higher than the value in the roots. However, the $^{42}K^+/^{137}Cs^+$ ratio in each leaf did not differ significantly, indicating that the primary transport of K^+ and Cs^+ in the shoots are similarly regulated. On the other hand, among the radionuclides stored in the roots over 4 h, 30% of the $^{42}K^+$ was exported from the roots over the following hour, while only 8% of $^{137}Cs^+$ was exported. In addition, within the xylem, K^+ was shown to travel slowly, whereas Cs^+ passed quickly through the roots into the shoots. In conclusion, very different transport patterns for the two ions were demonstrated in the root tissues.

Key words

selectivity, channel blocker, ion uptake, deficiency, live-imaging

Introduction

Radiocesium is a contaminant that reaches the food chain via plants. Along with other radionuclides, radiocesium can be generated by nuclear reactions and can be released into the environment as a consequence of nuclear tests or accidents in nuclear power plants. Once radiocesium pollutes the environment, especially cesium (Cs^+)-137 ($^{137}Cs^+$), it remains an environmental contaminant for a long time because of its 30-year half-life.

It has been strongly suggested that plants can absorb Cs^+ through a mechanism linked to the potassium (K^+) uptake system (White and Broadley 2000). K^+ is a macronutrient and is an alkali metal having some similar chemical properties to Cs^+. Soil naturally contains both K^+ and Cs^+, and usually the content of the stable Cs isotope, ^{133}Cs, is less than one thousandth of the K content in Japanese paddy and upland soils (Kamei-Ishikawa *et al.,* 2011). At the uptake stage in roots, an increased K^+ concentration in an external culture solution could reduce the Cs^+ uptake rate, indicating that K^+ and Cs^+ compete with each other (Zhu and Smolders 2000). Similarly, in experiments conducted at a variety of polluted fields, K^+ fertilization reduced the $^{137}Cs^+$ amount in plant tissues (Robison and Stone 1992; Lembrechts 1993; Nisbet *et al.,* 1993; Ohmori *et al.,* 2014). Furthermore, some K^+ transporters functioning in K^+ uptake have Cs^+ permeability (White and Broadley 2000, Hampton *et al.,* 2005).

Knowledge regarding Cs^+ transport within the plant body in relation to K^+ is limited compared with that on the Cs^+ uptake to the roots. To compare Cs^+ and K^+ transport, several researchers have measured the concentration of Cs^+ and K^+ in different organs based on the hypothesis that different transport systems should result in different concentration distributions in the plant, which would appear as a varied Cs^+/K^+ ratio among organs (Tsukada et al, 2002; Schneider *et al.,* 2008). Then, the Cs^+/K^+ ratio was found to be > 2-fold different among the organs in willows (Gommers *et al.,* 2000), maize (Schneider *et al.,* 2008), and coconut trees (Robison *et al.,* 2009). In broad bean, the net uptake rates of K^+ and $^{137}Cs^+$ in certain organs in a day were determined, and it was shown that, unlike K^+, $^{137}Cs^+$ accumulated preferentially in the roots (Zhu *et al.,* 2002). These reports indicate that Cs^+ and K^+ behave differently in the plant body. Nevertheless, the Cs^+

transport system could be related to the K^+ transport mechanism because K^+ availability could modify the Cs^+ concentration distribution (Robison *et al.*, 2009; Nobori *et al.*, 2014). Additionally, the radiocesium, $^{134, 137}Cs^+$, concentration in brown rice strongly correlated with the ratio of $^{40}K^+$:$^{134, 137}Cs^+$ in straw (Sekimoto *et al.*, 2014). The Cs^+ transport stage could consist of several phases, including subcellular compartmentalization, vascular transport and remobilization. Until now, the transport phase, which could cause different distribution patterns of K^+ and Cs^+, has not been identified.

In this study, $^{42}K^+$ and $^{137}Cs^+$ were exploited to characterize the similarities and differences in the short-term movement of K^+ and Cs^+ in rice plants. First, a $^{42}K^+$–$^{137}Cs^+$ double-tracer experiment to analyze the movement of K^+ and Cs^+ in the same sample was established. Then, the $^{42}K^+$–$^{137}Cs^+$ double-tracer technique was applied to investigate the competitive uptake and the long-distance vascular transport properties of K^+ and Cs^+ in terms of the K^+/Cs^+ ratio. Fluctuations of the K^+ and Cs^+ uptake rate in response to K conditions and the treatment of the K^+ transport inhibitors, tetraethyl ammonium (TEA) and gadolinium (Gd^{3+}), were also determined. The flow of K^+ and Cs^+ from the root tissues to the shoots was further investigated based on the sequential changes in the radionuclide contents in the roots and the leaves of intact seedlings, as determined by the live imaging data. Also, the behavior of $^{42}K^+$ and $^{137}Cs^+$ along the length of the root vascular tissue was characterized by tracking the concentration of each radionuclide in 1-cm-long root segments. To our knowledge, this is the first report presenting a direct contrast of internal K^+ and Cs^+ transport using their radionuclides as tracers.

Materials and Methods

Measurement of $^{42}K^+$ and $^{137}Cs^+$ by gamma-counting methods

The solution of ^{42}KCl was obtained using a $^{42}Ar^+$–$^{42}K^+$ generator (Homareda *et al.*, 1986; Aramaki *et al.*, 2015).

The gamma-ray emitted from $^{42}K^+$ (1525 keV) and $^{137}Cs^+$ (661.7 keV) (Fig. 1A) was measured by a well-type NaI (Tl) scintillation counter (NaI counter; ARC-300, Aloka, Tokyo, Japan) with the counting window set at 200−1600 keV.

When a sample contains both radioisotopes, the short half-life of $^{42}K^+$ (12.36 h) is exploited to determine the amount of $^{42}K^+$ by subtracting $^{137}Cs^+$ (counts per minute, cpm) from the total amount of $^{137}Cs^+$ and $^{42}K^+$ (cpm). The amount of $^{137}Cs^+$ (cpm) can be determined by measuring the sample after $^{42}K^+$ has decayed. To verify this "simple subtraction" method, the test sample solutions with or without $^{137}Cs^+$ (0, 80 or 890 Bq/ml) were prepared, to which $^{42}K^+$ at 120 Bq/ml or 640 Bq/ml was added (day 0). Then, 1 ml of each test solution was placed into a plastic tube (2 ml) and a U8 container (100 ml) to be analyzed using the NaI counter and a high purity germanium (Ge) detector (Ge detector; GEM-type, ORTEC), respectively. To the U8 container, 9 ml of pure water was added to stabilize the sample. The NaI counter and Ge detector measurements were performed at exactly the same time to eliminate an attenuation correction. The radioactivity was measured three times over an 8-day period, from day 0 to day 7, for an exact time to obtain enough counts to allow for counting error of less than 10%.

The amount of $^{42}K^+$ (Bq) in the test solution measured by the Ge detector was compared with the amount of $^{42}K^+$ (cpm) determined by the simple subtraction method.

Plant growth conditions

Rice (*Oryza sativa*. L. 'Nipponbare') seeds were germinated by submerging them in water at 30°C for 3 d. After germination, plantlets were put on plastic nets and floated on a 0.5 mM $CaCl_2$ solution at 30°C for 2 d. Then, rice plants were transplanted to the half-strength Kimura-B nutrient solution (270 μM K^+) supplemented with 0.1 μM CsCl. Cultivation occurred in the growth chamber set at 30°C and a light/dark cycle of 16 h/8 h. The concentrations of the chemicals in the solution was: 180 μM $(NH_4)_2SO_4$, 270 μM $MgSO_4$, 91 μM KNO_3, 180 μM $Ca(NO_3)_2$, 91 μM KH_2PO_4, 46 μM K_2SO_4, 46 μM Fe-citrate, 6.7 μM $MnCl_2$, 9 μM H_3BO_3, 150 nM $ZnSO_4$, 160 nM $CuSO_4$ and 15 nM $(NH_4)_6Mo_7O_{24}$. To keep the pH to 5.6, 2.5 mM 2-morpholinoethanesulfonic acid (MES), monohydrate, was added and adjusted by NaOH (~1 mM). The nutrient solution was refreshed every 2−3 d. Some seedlings were transplanted to the nutrient solution with low K (5 μM) or the one with high K (3 mM) concentration 4 days before the

experiment.

Measurement of K^+ and Cs^+ uptake rate

Two-week-old rice seedlings developing the fourth leaf (L4) were used for the radionuclide K^+ and Cs^+ uptake analysis. For the incubation medium, half-strength Kimura-B supplemented with 0.1 μM CsCl nutrient solution containing 10, 20, 100, 250, 1000 or 2000 μM K^+ was prepared, to which the 15−90 Bq/ml of $^{42}K^+$ as well as 25−50 Bq/ml of $^{137}Cs^+$ were added. To modify the K^+ concentration, potassium salt in the half-strength Kimura-B nutrient solution was substituted by a sodium salt, and then KCl was added at a concentration of 10−2000 μM.

The rice seedlings' roots were pre-incubated in the incubation medium without radionuclides at 30°C for 10 min, followed by a 20 min incubation in the incubation medium at 30°C. To measure the inhibition effects of TEA and Gd^{3+} on the K^+ and Cs^+ uptake, either 20 mM TEACl or 0.1 mM $GdCl_3$ was added to the incubation medium 3 min before the addition of radiotracers, and the incubation time was set at 15 min. After incubation, the seedlings fed with $^{42}K^+$ and $^{137}Cs^+$ were washed in the incubation solution with no radionuclide at 4°C for 10 min. Then, the seedlings were harvested, the roots and the shoots were separated, their fresh weight was measured, and the level of radionuclides was consequently counted using NaI counter with the counting window set at 200−1600 keV to measure the total gamma radiation (cpm) emitted by $^{42}K^+$ and $^{137}Cs^+$. Then, one week later, when $^{42}K^+$ had decayed below the detection limit, the gamma-rays of the samples were counted again to determine the $^{137}Cs^+$ radiation. Accordingly, the radiation emitted by $^{42}K^+$ was calculated from the data of total counts and $^{137}Cs^+$ counts by simple subtraction. The amounts of K^+ and Cs^+ accumulated in the roots and the shoots over ~20 min was calculated based on the amount of $^{42}K^+$ and $^{137}Cs^+$, as well as the concentration of K^+ (10−2000 μM) and Cs^+ (0.1 μM) in the incubation medium. Finally, the uptake rate was obtained by dividing the total accumulation by the root fresh weight and time.

Analysis of K^+ and Cs^+ distribution among the tissues by double-tracer technique

Three-week-old seedlings having six mature leaves (L1−L6) and one elongating

leaf (L7) were incubated in the half-strength Kimura-B medium supplemented with 0.1 μM CsCl nutrient solution containing 100 Bq/ml of $^{42}K^{+}$ and 3000 Bq/ml $^{137}Cs^{+}$ at 30°C for 30 min. After incubation, rice plants were washed in the incubation solution with no radionuclide at 4°C for 10 min. At harvesting, the roots, L4, L5, L6 and L7 were separated, and the remaining tissues, including old leaves (L1−L3) and the bottom of the shoots, were collected. L4, L5, and L6 were further separated into sheath and blade. L7, which was just elongating and hidden in the L6 sheath, had not developed a sheath yet. The radioactivity of $^{42}K^{+}$ and $^{137}Cs^{+}$ in each tissue was determined as described above, and the amount of K^{+} and Cs^{+} transported to each tissue in 30 min was calculated.

Root-to-shoot flow analysis using a live-imaging system

To analyze the K^{+} and Cs^{+} transport kinetics from the roots to the shoots, the radioactivity of $^{42}K^{+}$ and $^{137}Cs^{+}$ in the roots and the shoots was sequentially quantified using a real-time radioisotope imaging system (RRIS) (Kanno *et al*., 2012; Hirose *et al.*, 2013; Sugita *et al.*, 2014; Aramaki *et al.*, 2015). The roots of 10-day-old rice seedlings with developing L3s were placed in root chambers containing 3 ml of the half-strength Kimura-B medium supplemented with 0.1 μM CsCl nutrient solution. Then, the seedlings, as along with the root chambers, were placed on a detector surface 10 cm wide and 20 cm high. The roots in the root chambers were fixed using a blue polyurethane sheet. The sequential imaging was started immediately after the nutrient solution was replaced with the incubation medium containing either 9 kBq $^{42}K^{+}$ or 150 kBq $^{137}Cs^{+}$. During imaging, intermittent lighting with a light/dark cycle of 7 min/3 min was employed. The image of the radioactivity was captured during the dark period because the RRIS contains a charge coupled device camera, which is highly sensitive to photons (Hirose *et al.*, 2013). After 4 h, the incubation medium in the root chamber was replaced with the radionuclide-free medium, and the imaging was continued for another 4 h. For the quantitative analyses, the signal intensities detected in the regions-of-interest (ROIs) set as the roots and the shoots, as well as the medium and the background area, were measured using image analysis software (AQUACOSMOS, Hamamatsu Photonics, Co., Hamamatsu City, Japan). To describe the time course of the intensity in the roots and the shoots, the intensity

in each ROI was normalized by the intensity at 4 h. For $^{42}K^+$ quantification, the radioactive decay that occurred during imaging because of the short half-life was computationally corrected.

Analysis of K^+ and Cs^+ transport along the root vascular tissue

The 6-day-old seedlings having 6−7 cm long main roots and some crown roots shorter than 1 cm were laid in a compartment-box (Kawasaki *et al.*, 1984; Ma *et al.*, 2001; Kobayashi *et al.*, 2013). For the main roots, the segments between 2 cm and 3 cm from the root tip were partitioned using Vaseline containing the incubation medium supplemented with either 1 kBq $^{42}K^+$ or 1.6 kBq $^{137}Cs^+$. Other root parts were submerged in the nutrient solution without radionuclides. After 1 h of incubation, the radionuclide-added root section was excised, and the remaining roots were separated into bottom roots, upper roots, crown roots, and shoots. The amount of $^{42}K^+$ or $^{137}Cs^+$ in each tissue was determined using an imaging plate (BAS–IP-MS, GE Healthcare UK, Buckinghamshire, UK) and a FLA5000 image analyzer (FujiFilm, Tokyo, Japan). The signal intensities per tissue were calculated using image analysis software (Image Gauge version 4.0, FujiFilm).

Results

Development of the $^{42}K^+$–$^{137}Cs^+$ double-tracer technique

$^{42}K^+$ and $^{137}Cs^+$ were placed in one sample to achieve the simultaneous tracking of K^+ and Cs^+, which could provide direct evidence on their movements. To use $^{42}K^+$ and $^{137}Cs^+$ as double-tracers, a differential determination between $^{42}K^+$ and $^{137}Cs^+$ was needed. The decay modes of $^{42}K^+$ and $^{137}Cs^+$ are presented in Fig. 1A. Both radionuclides emit gamma rays, thus, the differential determination is easily realized by the Ge detector (Fig. 1B). However, the Ge detector is unfit for high-throughput measurements mainly due to the low counting efficiency. Thus, we determined if the NaI counter was suitable for the measurement of $^{42}K^+$ and $^{137}Cs^+$. Generally, the energy resolution of the NaI counter is lower than the Ge detector, which could be a drawback to using the NaI counter. Thus, another method based on the large difference in the half-lives of the two radionuclides

(Fig. 1A) was tested. When both $^{42}K^+$ and $^{137}Cs^+$ are contained in a sample, there should be a gap between the total radioactivity measured at sampling and the radioactivity measured several days after. This gap is caused by the radioactive decay of $^{42}K^+$ (Fig. 1B). Accordingly, determining the amount of $^{42}K^+$ and $^{137}Cs^+$ individually in a sample using the NaI counter could be performed using the simple subtraction equation, "sum($^{42}K^+$ and $^{137}Cs^+$) − $^{137}Cs^+$ = $^{42}K^+$". The validity of this method was investigated by comparing the calculated amount of $^{42}K^+$ (cpm) and the $^{42}K^+$ amount (Bq) determined by the Ge detector (Fig. 1C). Then, it was shown that the $^{42}K^+$ amount (cpm) estimated by the simple subtraction method correlated well (R^2 > 0.99) with the $^{42}K^+$ amount (Bq), regardless of the amount of $^{137}Cs^+$ coexisting in the sample. Thus, the $^{42}K^+$–$^{137}Cs^+$ double-tracer method, in combination with the quantitative determination using the NaI counter, was applied to our physiological study.

Properties of K^+ and Cs^+ uptake by roots

The K^+ uptake kinetics of 2-week-old rice plants grown in the standard nutrient solution containing 270 μM K^+ was determined. As the K^+ concentration in the soaking medium increased, the K^+ uptake rate increased until the K^+ concentration in the medium reached 1,000 μM (Fig. 2A). The K_m value for K^+ absorption was estimated to be ~50 μM. When the K^+ concentration in the external medium was higher than 1,000 μM, the K^+ uptake rate did not increase, while the uptake rate of Cs^+ from the medium containing 0.1 μM Cs^+ was still competitively reduced from 0.048 ± 0.0030 to 0.033 ± 0.0026 (pmol/mg root/20 min) (Fig. 2A). However, when the external K^+ concentration decreased from 100 μM to 10 μM, the Cs^+ uptake rate only showed 2.7-fold increase, from 0.26 ± 0.034 to 0.72 ± 0.064 (pmol/mg root/20 min) (Fig. 2A). Therefore, K^+ in the medium did not appear to act by simply competing with Cs^+ uptake in a manner that was linearly related to the external concentration. To characterize the properties of K^+ transport against Cs^+, the $^{42}K^+/^{137}Cs^+$ selectivity factor was calculated (Fig. 2B). Here, the $^{42}K^+/^{137}Cs^+$ selectivity factor was defined as:

$$^{42}K^+/^{137}Cs^+ \text{ selectivity factor} =$$

$$\frac{\text{K}^+ \text{ uptake rate / Cs}^+ \text{ uptake rate}}{\text{K}^+ \text{ concentration in medium/ Cs}^+ \text{ concentration in medium}}.$$

A unity of the $^{42}K^+/^{137}Cs^+$ selectivity factor indicates that the roots absorb Cs^+ indistinctively from K^+, as if Cs^+ mimics K^+ uptake perfectly. The $^{42}K^+/^{137}Cs^+$ selectivity factor was found to be ~7 under low K^+ concentration (~20 μM), and 11~ under K^+ concentrations between 250 μM and 1 mM (Fig. 2B). Thus, it was hypothesized that at least two distinct mechanisms for K^+ acquisition, having different $^{42}K^+/^{137}Cs^+$ selectivity factors, coexisted in the roots of rice grown in 270 μM K^+. At 2 mM K condition, the $^{42}K^+/^{137}Cs^+$ selectivity factor was decreased largely due to the saturated K^+ uptake rate. In addition, the Cs^+ uptake rate showed only 30% decrease while the K concentration in the solution was doubled, from 1 mM to 2 mM. It can be supposed that there is a membrane transport system with Cs^+ specific affinity which does not diminish Cs^+ permeability even under the high K condition.

The effect of low-K and high-K treatments and the K transport inhibitors on the uptake of K^+ and Cs^+

To consider the molecular mechanisms determining the K^+ and Cs^+ uptake rate, the effect of the K status in the growth condition was investigated using the rice plants transplanted from normal K condition (270 μM) to either low-K (5 μM) or high-K (3 mM) condition 4 days before the experiment. Then, both the K^+ and Cs^+ uptake rates tended to be increased in response to the low-K treatment, and to be decreased by the high-K treatment, although the low-K treatment affected the K uptake rate less significantly (Table 1). This result supports the current view that the Cs^+ absorption can be mediated by certain K^+ transport system, at least partially, which can be modulated by the environmental K condition (Zhu and Smolders 2000). In rice plants, the K transport system in the seedlings cultivated in 3 mM K was shown to be different from that in 270 μM K (Nobori *et al*. 2014), and thus 3 mM K could be regarded as high-K. On the other hand, cultivation at the K concentrations less than 27 μM K would be effective to alter the Cs behavior (Nobori *et al*. 2015) presumably as a result of the transition of the K transport systems to adapt the low-K condition. Therefore, cultivation in 5 μM K

was thought to be adequate to investigate the ion transport system functioning in low-K condition. A significant reduction of the $^{42}K^+/^{137}Cs^+$ selectivity factor in response to the low-K condition was found under both 20 μM and 1 mM K (Table 1). On the other hand, the high-K treatment had little influence on the $^{42}K^+/^{137}Cs^+$ selectivity factor (Table 1). Therefore, it was suggested that the increased uptake rate of K^+ and Cs^+ in response to the low-K condition was caused by the up-regulation of specific K^+ transporter(s) having relatively low K^+ selectivity over Cs^+. Unlike the low-K treatment, the high-K condition was supposed to uniformly reduce the molecules mediating K^+ and Cs^+ absorption, thus the $^{42}K^+/^{137}Cs^+$ selectivity factor could not be changed.

The nature of the molecule(s) transporting K^+ and Cs^+ in the control condition was further investigated by determining the effect of the channel blockers. Treatment with 20 mM TEA, the K^+-selective channel blocker, tended to reduce the K^+ uptake rate, but the effect was not significant (Table 1). The uptake rate of Cs at the external Cs concentration of 0.1 μM was decreased by the TEA treatment to 45.8% of the control in the presence of 20 μM K, while it showed no significant decrease when the external K^+ concentration was 1 mM (Table 1). Consequently, the $^{42}K^+/^{137}Cs^+$ selectivity factor was increased from 5.46 to 7.59 by the TEA treatment in the presence of 20 μM K (Table 1). On the other hand, Gd^{3+} treatment showed hardly no effect on the K^+ and Cs^+ uptake regardless of the external K concentration. Thus, the contribution of the non-selective cation channel (NSCC) in the K^+ and Cs^+ uptake was supposed to be scarce in the rice plant grown with 270 μM K.

Long-distance transport properties of K^+ and Cs^+ along the vascular tissues

Following the roots' acquisition, the K^+ and Cs^+ distribution process along the vascular tissue was comparatively characterized. As a basis for comparison, the roots of 3-week-old rice seedlings were treated with $^{42}K^+$ and $^{137}Cs^+$ for 30 min, and the amount of K^+ and Cs^+ transported to the root, L4, L5, L6, L7, and other shoot tissues via the vascular tissue was measured. The K^+/Cs^+ ratio of each organ was then determined (Table 2). Within 30 min of the experiment, the rice roots accumulated 3,559 nmol/g K^+ and 262.6 pmol/g Cs^+, while the shoots accumulated 479 nmol/g K^+ and 8.3 pmol/g Cs^+ in total (Table 2). Thus, the

K^+/Cs^+ ratios in the roots and the shoots were 1.35×10^4 and 5.86×10^4, respectively (Table 2). The 4.28-times higher K^+/Cs^+ ratio in the shoots than in the roots (Table 2) could indicate that the root-to-shoot K^+ transfer mechanism is a further barrier to Cs^+ penetration into the plants, along with the selective K^+ uptake in the roots. An alternative explanation for the high K^+/Cs^+ ratio in the shoots is that different flow rates exist for K^+ and Cs^+ in root tissues. If K^+ could enter the shoot earlier than Cs^+, an increased K^+/Cs^+ ratio would be present, especially at the beginning of the experiment.

The K^+/Cs^+ ratios among the shoot tissues, which ranged from 3.72 to 5.79 relative to the root, were not significantly different (Table 2). Therefore, the two ions should have moved after they reached the shoot tissue, at least before the ions were pooled in the shoot tissues. L7 was the newest immature leaf that was expected to receive its nutrient supply via the phloem. Given that the K^+/Cs^+ ratio in L7 was similar to other mature shoot tissues, the xylem-to-phloem transfer process of Cs^+ may have occurred in the primary K^+ transport pathway, providing little K^+/Cs^+ discrimination. Nevertheless, the ratio of the sheath K^+/Cs^+ ratio to the blade K^+/Cs^+ ratio was above unity in all leaves (Table 2).

Kinetics of the root-to-shoot flow of K^+ and Cs^+

To further characterize the different transport properties of K^+ and Cs^+ in root tissues, the flow of K^+ and Cs^+ from the root to the shoot was investigated based on the sequential quantification data derived from the radionuclide imaging study. Four rice plants were placed on the surface of a real-time radioisotope imaging system (RRIS) and either $^{42}K^+$ or $^{137}Cs^+$ was introduced through the roots for 4 h (Fig. 3A). The RRIS monitored the root uptake kinetics and transport status to the shoots. Then, the uptake medium was exchanged to the nutrient solution without radionuclides for another 4 h so that the movement of $^{42}K^+$ and $^{137}Cs^+$ that had been stored in the root tissues could be traced (Fig. 3B). This experimental procedure illustrated the ion flow from the roots to other tissues without affecting the ion dynamics in the seedlings. In the leaves, the increased uptake rates of $^{42}K^+$ and $^{137}Cs^+$ were proportional to the time rates between 3 and 5 h (Fig. 3C), indicating that their concentrations in the xylem stream were constant during this period. Thus, the concave upward signal intensities found in $^{42}K^+$ before 3 h and in

$^{137}Cs^+$ before 1 h (Fig. 3C) may represent the gradually rising concentrations of $^{42}K^+$ and $^{137}Cs^+$, respectively, in the xylem stream. Conversely, the observation that the increase in the signal rate was slightly reduced after 5 h (Fig. 3C) may have resulted from a concentration reduction because of the influx of the non-labeled K^+ and Cs^+ into the roots. Based on these considerations, the changes in the signal intensities in only the roots between 4 and 5 h were regarded as the xylem loading efficiency of K^+ and Cs^+ in the roots. The $^{42}K^+$ signals found in the roots at 4 h declined to 70% within 1 h, whereas less than 8% of the $^{137}Cs^+$ signals were lost (Fig. 3D). Even after 8 h of imaging, the roots maintained ~90% of the $^{137}Cs^+$ signals accumulated over 4 h (Fig. 3D). These observations indicate that the capacity of the exchangeable $^{137}Cs^+$, presumably cytosolic $^{137}Cs^+$, in the root tissues was small at 4 h and was rapidly transported to the shoots within the next hour. K^+ was shown to turn over at a high rate, while Cs^+ could be efficiently trapped in the root tissues. This characteristic movement of K^+ and Cs^+, rather than different flow rates in the roots, could lead to the higher K^+/Cs^+ ratio found in the shoot tissues (Table 2).

K^+ and Cs^+ behaviors during vascular transport within the roots

The long-distance K^+ and Cs^+ transport systems within the root vascular bundles were additionally investigated by tracking the $^{42}K^+$ and $^{137}Cs^+$ after they were added to the 1-cm-long segments of the main root. The radionuclide absorption period was set to be 1 h, considering that a linier uptake and an unidirectional transport were observed for several ions at least until 3 h of the radionuclide introduction from the root (Kobayashi *et al.* 2013).

When $^{42}K^+$ was added to a root segment for 1 h, 77% of $^{42}K^+$ was found in the radionuclide-added segment (Fig. 4A). Of the remaining 23%, which was translocated to other tissues through the vascular bundle, 75% was distributed in the upper roots and only 15% reached the shoots (Fig. 4B). However, the proportion of $^{137}Cs^+$ transported out of the radionuclide-added segment was only 8% (Fig. 4A). Furthermore, unlike the $^{42}K^+$ distribution, the percentage of $^{137}Cs^+$ distributed to the upper roots was no more than 20% (Fig. 4B). A previous report showed that the distribution ratio of shoots:upper-roots within hours differed from element to element (Kobayashi *et al*., 2013). Thus, the ion transport in the root

vascular tissue may be regulated individually, presumably for physiological reasons. Given that Cs^+ is rather toxic to plants, especially at high concentrations (Hampton *et al.,* 2004), the retrieval of Cs^+ from the xylem stream, as suggested for Na^+ to protect the leaves from saline conditions (Horie *et al.,* 2005), is assumed to be beneficial to the plant. However, at least in the rice plants used in this study, the opposite was found. K^+ tended to travel through the root vascular tissues slowly, whereas Cs^+ passed quickly through the root vascular bundles to the shoots.

Discussion

The roots of rice grown in the complete nutrient solution containing 270 μM K^+ and 0.1 μM Cs^+ revealed the saturable uptake of K^+ (Fig. 2A). It was striking that the $^{42}K^+/^{137}Cs^+$ selectivity decreased drastically when the K^+ concentration in the soaking medium was below 20 μM (Fig. 2B), and decreased even more in response to the K deficient condition (Table 1). The loss of discrimination between K^+, Rb^+, and Cs^+ during the root uptake stage has been observed in K-starved rice, which could involve KT/HAK/KUP transporters (Bañuelos *et al.*, 2002). In *Arabidopsis*, AtHAK5, a high-affinity K^+ transporter localized in root epidermal cells, mediates the K^+ influx to the root cells from areas of low K^+ concentration and also regulates Cs^+ uptake (Gierth *et al.,* 2005; Qi *et al.,* 2008). Until now, the primary K^+ transporters or K^+ channels that function in K^+ absorption in rice roots has not been fully characterized. Eight rice KUP/HAK/KT transporters exist in the same cluster as AtHAK5 (Véry *et al.*, 2014). Among them, OsHAK1 and OsHAK5 may function in K^+ uptake in the roots (Bañuelos *et al.*, 2002; Horie *et al.*, 2011). In the roots of rice plant cultured in 270 μM K, the weak induction of *OsHAK1* expression was observed (unpublished data), although its involvement in Cs^+ uptake is not clear. In this study, the participation of the TEA-sensitive K channel in the root K^+ uptake was not observed apparently (Table 1). Hence, it can be assumed that the degree of decline in the K uptake rate caused by the TEA treatment is different depending on the plant species. In *Arabidopsis*, the transient treatment of 10 mM TEA drastically reduced the net flux of K^+, to almost one fifth of the non-treated sample (Ten Hoopen et al. 2010).

In contrast, the addition of 30 mM TEA to the culture solution showed no effect on the K content in the indica rice (Liu et al. 2006). In the case of pepper, the balance between the K^+ release and the K^+ uptake was disrupted by the 20 mM TEA treatment, and subsequently resulted in the 51% reduction in the net K uptake during 5 h (Pacheco-Arjona et al., 2011). Taken these things into consideration, the K uptake mechanism in rice roots could be regarded as a whole as a system relatively insensitive to TEA. Nevertheless, there could be a K transport apparatus whose function could be blocked by TEA. Indeed, up to 50% of the Cs uptake is found to be dependent on the TEA-sensitive K^+-channels (Table 1). It could be assumed that contribution of these molecules to the total uptake of K could be too small to be detected in this study. It could also be suggested that the high affinity K uptake system functioning in the low K concentration is composed of more than 2 systems having different sensitivity to TEA and different Cs permeability. The participation of NSCCs in K^+ and Cs^+ uptake was not observed in the rice root (Table 1). It is thought that it is not due to 0.1 mM Gd^{3+} insufficiency to block the NSCC activity, nor because of NSCCs not functioning in the surface of the rice root. In fact, the same experiment using 0.1 mM Gd^{3+} showed considerable reduction in the Mg^{2+} uptake rate, to one third of the non-treated control (unpublished data). Additionally, contrary to the previous indication (Zhu and Smolders 2000), the competitive effect of K^+ on the Cs^+ uptake even at a K^+ concentration higher than 1,000 μM was clearly demonstrated by the application of $^{42}K^+$–$^{137}Cs^+$ double-tracer (Fig. 2A). The previous studies have evaluated the K/Cs discrimination in the root based on the total content of K and Cs in the plant body at the certain time point (Zhu and Smolders 2000). It may be possible that the long-term culture in the higher K concentration promoted the efflux of K^+, resulting in the reduction in the K/Cs value in the net uptake amount (influx – efflux). Additionally, long duration of the study can affect the plant biomass and subsequently cause a dilution effect on the mineral content, which can lead the erroneous recognition of the mineral uptake activity and transport direction. In the short-term radiotracer experiment we have performed, there is no need to consider the biomass dilution effect. The ion uptake activity and the transport property can be directly calculated based on the net flux of the radiotracers in each tissue.

In regard to the distribution of K^+ and Cs^+ within plant, a previous report indicated that Cs^+ tended to accumulate in rice roots when compared with K^+ during harvesting season (Tsukada *et al.,* 2002). Here, K^+ and Cs^+ were demonstrated to move differentially soon after they entered the root tissues and before reaching the xylem. Cs^+ was retained in the root tissues with high efficiency, while K^+ was easily exchanged and transported toward the shoots (Fig. 3D). The flexible turnover of cytosolic K^+ ($t_{1/2}$ = 21−27 min) was suggested by a flux analysis using $^{42}K^+$ in barley roots grown in 112.5 μM K^+ (Kronzucker *et al.,* 2003). The movement of K^+ from the cortical cells to the stellar cells through the symplast may be driven by a concentration gradient (De Boer 1999). A conceivable mechanism for the different movement rates of K^+ and Cs^+ is vacuolar compartmentalization in the symplast. It may be noteworthy that the QTLs identified as regulating the Cs^+ concentration, but not the K^+ concentration, included the gene encoding AtCHX20, a cation/proton antiporter in *Arabidopsis* (Kanter *et al.,* 2010), which localizes the endomembrane and has an ion transport specificity of $Cs^+ > Rb^+ > K^+$ when expressed in *E. coli* (Chanroj *et al.,* 2011). Furthermore, the SNARE protein Sec22p/SEC22 was found to specifically impact Cs^+ accumulation as a consequence of the Cs^+ deposition to the vacuole (Dräxl *et al.,* 2013). Also, it should be noted that the preferential accumulation of Cs^+ in root tissues can be affected by the environmental K^+ concentrations. Indeed, cultivation at various K conditions specifically affected the both Cs^+ uptake and Cs^+ allocation within the rice plants (Nobori *et al.* 2015). Therefore, the behavior of Cs^+ presented in this study can be differed in different K conditions.

After the ions pass through the root cells, they can be loaded into the xylem. K^+ and Cs^+ loading involves a shaker-type outward-rectifying channel named SKOR (Gaymard *et al.,* 1998). The activity of SKOR can be inhibited by abscisic acid through transcription reduction (Gaymard *et al.,* 1998; Tester 1999; Roberts and Snowman 2000), but could be stimulated by salinity-induced depolarization to mitigate the drastic decline of the K^+/Na^+ ratio in xylem sap (Maathuis and Amtmann 1999; Shabala *et al.,* 2010). K^+ in the xylem stream may influence the radial water flow within the xylem conduits by increasing the pore size of the intervessel pit membrane (Nardini *et al.,* 2011). In this regard, the possibility that K^+ itself travels between the xylem vessels exists, which may relate to the

observation that K^+ travels in the upper roots slowly (Fig. 4B). Alternatively, K^+ resorption from the xylem stream could be efficiently occurring in the surrounding cells through the K^+ transporters. This possibility is supported by a previous report describing the extensive expression of K^+ inward-rectifying channels in the plasma membrane of xylem parenchyma cells in barley roots (Wegner *et al.*, 1994).

The translocation of Cs^+ has long been suggested to occur less than K^+ based on the observation that, in mature rice plants, older leaves contain more Cs^+ while younger leaves contain more K^+ (Tsukada *et al.,* 2002). Our results showed a similar transport pattern for K^+ and Cs^+ in both the old and young leaves within 30 min after uptake through the roots (Table 2), highlighting the potential differential redistribution of K^+ and Cs^+ after the ions were pooled in the leaf tissues. Thus, the reduced translocation of radiocesium from non-edible aerial plant parts via the phloem could be effective in preventing radiocesium accumulation in the edible portions of crops (Nobori *et al.,* 2014). AKT2/3 K^+ channels in Arabidopsis (Deeken *et al.,* 2002) and KZM1 in maize (Philippar *et al.,* 2003) have been shown to contribute to the phloem K^+-loading process, but any roles in Cs^+ transport have not been discovered.

In conclusion, the different behaviors of K^+ and Cs^+ appeared at the beginning of their long-distance transport in rice seedlings. The large difference between K^+ and Cs^+ was found in their movement within the root tissues before reaching the shoots. These results imply the possibility of molecular breeding for developing the low Cs crops or, conversely, the variations applicable for Cs phytoremediation which accumulate radiocesium intensively to the up-ground shoot parts without disruption of K homeostasis in plants. Further characterization of the membrane transport process regulating the Cs accumulation in the root can allow the efficient breeding. The step-by-step analysis of ion transport using radionuclides described in this report could be a useful tool to characterize the *in planta* functions of each transporter and channel.

Acknowledgements

Authors thank to Ms. Sophie-Asako Xerri for her assisting the experiment and proofreading. This work was partially supported by a grant from the Ministry of Agriculture, Forestry, and Fisheries of Japan (Genomics-based Technology for Agricultural Improvement, LCT0002).

References

Aramaki T, Sugita R, Hirose A, Kobayashi NI, Tanoi K, Nakanish TM (2015) Application of ^{42}K to *Arabidopsis* tissues using real-time radioisotope imaging system (RRIS). *Radioisotopes* **64,** 169–176.

Ban˜ uelos MA, Garciadeblas B, Cubero B, Rodrı´guez-Navarro A (2002) Inventory and functional characterization of the HAK potassium transporters of rice. *Plant Physiology* **130,** 784–795.

De Boer AH (1999) Potassium Translocation into the Root Xylem. *Plant Biology* **1:**36–45

Deeken R, Geiger D, Fromm J, Koroleva O, Ache P, Langenfeld-Heyser R, Sauer N, May ST, Hedrich R (2002) Loss of the AKT2/3 potassium channel affects sugar loading into the phloem of *Arabidopsis*. *Planta* **216,** 334–344.

Dräxl S, Müller J, Li WB, Michalke B, Scherb H, Hense BA, Tschiersch J, Kanter U, Schäffner AR (2013) Caesium accumulation in yeast and plants is selectively repressed by loss of the SNARE Sec22p/SEC22. *Nature Communications* **4,** 2092. DOI:10.1038/ncomms3092

Gaymard F, Pilot G, Lacombe B, Bouchez D, Bruneau D, Boucherez J, Michaux-Ferriere N, Thibaud JB, Sentenac H (1998) Identification and disruption of a plant shaker-like outward channel involved in K1 release into the xylem sap. *Cell* **94,** 647–655.

Gierth M, Maser P, Schroeder J (2005) The potassium transporter AtHAK5 functions in K^+ deprivation-induced high affinity K^+ uptake and AKT1 K^+ channel contribution to K^+ uptake kinetics in Arabidopsis roots. *Plant Physiology* **137,** 1105–1114.

Gommers A, Thiry Y, Vandenhove H, Vandecasteele CM, Smolders E, Merckx R (2000) Radiocesium uptake by one-year-old willows planted as short rotation coppice. *Journal of Environmental Quality* **29,** 1384–1390.

Hampton CR, Bowen HC, Broadley MR, Hammond JP, Mead A, Payne KA, Pritchard J, White PJ (2004) Cesium Toxicity in *Arabidopsis*. *Plant Physiology* **136,** 3824–3837.

Hampton CR, Broadley MR, White PJ (2005) Short review: the mechanisms of radiocaesium uptake by Arabidopsis roots. *Nukleonika* **50,** (Supplement

1):S3−S8.

Hirose A, Yamawaki M, Kanno S, Igarashi S, Sugita R, Ohmae Y, Tanoi K, Nakanishi TM (2013) Development of a ^{14}C detectable real-time radioisotope imaging system for plants under intermittent light environment. *Journal of Radioanalytical and Nuclear Chemistry* **296,** 417–422.

Homareda H, Matsui H (1986) Biochemical utilization of ^{42}Ar-^{42}K Generator. *Radioisotopes* **35,** 543–546.

Horie T, Sugawara M, Okada T, Taira K, Kaothien-Nakayama P, Katsuhara M, Shinmyo A, Nakayama H (2011) Rice sodium-insensitive potassium transporter, OsHAK5, confers increased salt tolerance in tobacco BY2 cells. *Journal of Bioscience Bioengineering* **111,** 346–56.

Kamei-Ishikawa N, Tagami K, Uchida S (2011) Relationships among ^{137}Cs,^{133}Cs, and K in plant uptake observed in Japanese agricultural fields. *Journal of Radioanalytical and Nuclear Chemistry* **290,** 247–252.

Kanno S, Yamawaki M, Ishibashi H, Kobayashi NI, Hirose A, Tanoi K, Nussaume L, Nakanishi TM (2012) Development of real-time radioisotope imaging systems for plant nutrient uptake studies. *Philosophical Transactions of the Royal Society B* **367,** 1501–1508.

Kanter U, Hauser A, Michalke B, Dräxl S, Schäffner AR (2011) Cesium and strontium accumulation in shoots of *Arabidopsis thaliana*: genetic and physiological aspects. *Journal of Experimental Botany* **61,** 3995–4009.

Kawasaki T, Moritsugu M, Shimizu G. (1984) The absorption and translocation of ions in excised barley roots: A multicompartment transport box experiment. *Soil Science and Plant Nutrition* **30,** 417–425.

Kobayashi NI, Iwata N, Saito T, Suzuki H, Iwata R, Tanoi K, Nakanishi TM (2013) Different magnesium uptake and transport activity along the rice root axis revealed by ^{28}Mg tracer experiments. *Soil Science and Plant Nutrition* **59,** 149–155.

Kronzucker HJ, Szczerba MW, Britto DT (2003) Cytosolic potassium homeostasis revisited: ^{42}K-tracer analysis in *Hordeum vulgare* L. reveals set-point variations in $[K^+]$ Planta 217, 540–546.

Lembrechts J (1993) A review of literature on the effectiveness of chemical amendments in reducing the soil-to-plant transfer of radiostrontium and

radiocaesium. *Science of the Total Environment* **137,** 81–98.

Liu H-Y, Sun W-N, Su W-A, Tang Z-C (2006) Co-regulation of water channels and potassium channels in rice. *Physiologia Plantarum* **128,** 58–69.

Ma JF, Goto S, Tamai K, Ichii M (2001) Role of root hairs and lateral roots in silicon uptake by rice. *Plant Physiology* **127,** 1773–1780.

Nardini A, Salleo S, Jansen S (2011) More than just a vulnerable pipeline: xylem physiology in the light of ion-mediated regulation of plant water transport. *Journal of Experimental Botany* **62,** 4701–4718.

Nisbet AF, Konoplev AV, Shaw G, Lembrechts JF, Merckx R, Smolders E, Vandecasteele CM, Lönsjö H, Carini F, Burton O (1993) Application of fertilisers and ameliorants to reduce soil to plant transfer of radiocaesium and radiostrontium in the medium to long term — a summary. *Science of the Total Environment* **137,** 173–182, doi: 10.1016/0048-9697(93)90386-K

Nobori T, Kobayashi NI, Tanoi K, Nakanishi TM (2014) Effects of potassium in reducing the radiocesium translocation to grain in rice. *Soil Science and Plant Nutrition* **60,** 772–781.

Nobori T, Kobayashi NI, Tanoi K, Nakanishi TM (2015) Alteration in caesium behavior in rice caused by the potassium, phosphorous, and nitrogen deficiency. *Journal of Radioanalytical and Nuclear Chemistry, in press*

Ohmori Y, Kajikawa M, Nishida S, Tanaka N, Kobayashi NI, Tanoi K, Furukawa J, Fujiwara T (2014) The effect of fertilization on cesium concentration of rice grown in a paddy field in Fukushima Prefecture in 2011 and 2012. *Journal of Plant Research* **127,** 67–71.

Qi Z, Hampton CR, Shin R, Barkla BJ, White PJ, Schachtman DP (2008) The high affinity K^+ transporter AtHAK5 plays a physiological role in planta at very low K^+ concentrations and provides a caesium uptake pathway in *Arabidopsis*. *Journal of Experimental Botany* **59,** 595–607.

Pacheco-Arjona JR, Ruiz-Lau N, Medina-Lara F, Minero-García Y, Echevarría-Machado I, De los Santos-Briones C and Martínez-Estévez M (2011) Effects of ammonium nitrate, cesium chloride and tetraethylammonium on high-affinity potassium uptake in habanero pepper plantlets (*Capsicum chinense* Jacq.). *African Journal of Biotechnology* **10,** 13418-13429.

Philippar K, Büchsenschütz K, Abshagen M, Fuchs I, Geiger D, Lacombe B,

Hedrich R (2003) The K^+ channel KZM1 mediates potassium uptake into the phloem and guard cells of the C4 grass *Zea mays*. *Journal of Biological Chemistry* **278,** 16973–16981. doi: 10.1074/jbc.M212720200

Roberts SK, Snowman BN (2000) The effects of ABA on channel-mediated K^+ transport across higher plant roots. *Journal of Experimental Botany* **51,** 1585–1594.

Robison WL, Brown PH, Stone EL, Hamilton TF, Conrado CL, Kehl S (2009) Distribution and ratios of ^{137}Cs and K in control and K-treated coconut trees at Bikini Island where nuclear test fallout occurred: effects and implications. *Journal of Environmental Radioactivity* **100,** 76–83.

Robison WL, Stone EL (1992) The effect of potassium on the uptake of ^{137}Cs in food crops grown on coral soils: coconut at Bikini Atoll. *Health Physics* **62,** 496–511.

Schneider K, Kuznetzov VK, Sanzharova NI, Kanter U, Telikh KM, Khlopuk MS. (2008) Soil-to-plant and soil-to-grain transfer of ^{137}Cs in field-grown maize hybrids during two contrasting seasons: assessing the phenotypic variability and its genetic component. *Radiation and Environmental Biophysics* **47,** 241–252.

Sekimoto H, Yamada T, Hotsuki T, Fujiwara T, Mimura T, Matsuzaki A (2014) Evaluation of the radioactive Cs concentration in brown rice based on the K nutritional status of shoots. *Journal of Plant Research* **127,** 73–78.

Shabala S, Shabala S, Cuin TA, Pang J, Percey W, Chen Z, Conn S, Eing C, Wegner LH (2010) Xylem ionic relations and salinity tolerance in barley. *Plant Journal* **61,** 839–853.

Sugita R, Kobayashi NI, Hirose A, Tanoi K, Nakanishi TM (2014) Evaluation of in vivo detection properties of ^{22}Na, ^{65}Zn, ^{86}Rb, ^{109}Cd and ^{137}Cs in plant tissues using real-time radioisotope imaging system. *Physics in Medicine and Biology* **59,** 837–851.

Sunarpi, Horie T, Motoda J, Kubo M, Yang H, Yoda K, Horie R, Chan W-Y, Leung H-Y, Hattori K, Konomi M, Osumi M, Yamagami M, Schroeder JI, Uozumi N (2005) Enhanced salt tolerance mediated by AtHKT1 transporter-induced Na^+ unloading from xylem vessels to xylem parenchyma cells. *Plant Journal* **44,** 928–938.

Ten Hoopen F, Cuin TA, Pedas P, Hegelund JN, Shabala S, Schjoerring JK, Jahn TP (2010) Competition between uptake of ammonium and potassium in barley and *Arabidopsis* roots: molecular mechanisms and physiological consequences. *Journal of Experimental Botany* **61,** 2303–2315.

Tester M (1999) Control of long-distance K^+ transport by ABA. *Trends in Plant Science* **4,** 5–6.

Tsukada H, Hasegawa H, Hisamatsu S, Yamasaki S (2002) Rice uptake and distributions of radioactive ^{137}Cs, stable ^{133}Cs and K from soil. *Environmental Pollution* **117,** 403–409.

Véry A-A, Nieves-Cordones M, Daly M, Khan I, Fizames C, Sentenac H (2014) Molecular biology of K(+) transport across the plant cell membrane: What do we learn from comparison between plant species? *Journal of Plant Physiology* **171,** 748–769.

Wegner LH, De Boer AH, Raschke K (1994) Properties of the K^+ inward rectifier in the plasma membrane of xylem parenchyma cells from barley roots: effects of TEA^+, Ca^{2+}, Ba^{2+} and La^{3+}. *Journal of Membrane Biology* **142,** 363–379.

White PJ, Broadley MR (2000) Mechanisms of caesium uptake by plants. *New Phytologist* **147,** 241−256.

Zhu Y-G, Shaw G, Nisbet AF, Wilkins BT (2002) Effect of external potassium supply and plant age on the uptake of radiocaesium (^{137}Cs) by broad bean (*Vicia faba*): interpretation of results from a large-scale hydroponic study. *Environmental and Experimental Botany* **47,** 173–187.

Zhu Y-G, Smolders E (2000) Plant uptake of radiocaesium: a review of mechanisms, regulation and application. *Journal of Experimental Botany* **51,** 1635–1645.

Table 1

The impact of the growth condition and the addition of the K transport inhibitor on the uptake rate of K^+ and Cs^+, and the $^{42}K^+/^{137}Cs^+$ selectivity factor. The incubation solutions contained either 20 μM or 1 mM K. The concentration of Cs was always 0.1 μM. The samples were grown under either normal conditions (270 μM K, control), low K (5 μM K) or high K (3 mM K) conditions during 4 days preceding the experiment. The values are means ± SD (n = 4). The effect of 20 mM TEA or 0.1 mM Gd^{3+} was presented as the modulated uptake rate (% of the control). Single and double asterisks denote significant differences from the control values at a *p* of < 0.05 and < 0.01, respectively, via Welch's two-sample t-test.

	K concentration					Growth condition						Inhibitor treatment			
	in incubation solution	Control				Low K			High K			TEA		Gd^{3+}	
K uptake rate	20 μM	1.54	±	0.313		2.02	±	0.181	* 0.535	±	0.0638	72.3%		108%	
(nmol/mg/30min)	1 mM	11.7	±	2.27	*	18.0	±	1.06	* 3.56	±	0.311	79.1%		92.6%	
Cs uptake rate	20 μM	1.44	±	0.423	*	2.84	±	0.279	* 0.353	±	0.104	** 45.8%		76.6%	
(pmol/mg/30min)	1 mM	0.0985	±	0.0133	**	0.256	±	0.00515	** 0.0448	±	0.00744	91.5%		94.7%	
Selectivity factor	20 μM	5.46	±	0.771	*	3.58	±	0.434	7.87	±	1.41	* 7.59	± 0.599	7.31	± 2.93
	1 mM	11.8	±	0.976	**	7.05	±	0.432	8.13	±	1.79	11.3	± 0.936	12.8	± 1.48

Table 2

Distribution of potassium (K^+, nmol/g) and cesium (Cs^+, pmol/g) in rice tissues. Ion concentrations were obtained based on their concentration in external solution, 270 μM K^+ and 0.1 μM Cs^+, and the radioactivity in the tissues. Then, the K^+/Cs^+ ratio of each tissue, along with the relative K^+/Cs^+ ratio normalized by the root, and the ratio of the sheath K^+/Cs^+ ratio to the blade K^+/Cs^+ ratio after the roots were exposed for 30 min to a nutrient solution, were calculated. The values are means with SD (n = 5).

			Biomass			Concentration						K/Cs								
			(mg F.W.)			K (nmol/g)			Cs (pmol/g)			K/Cs (mol/mol)		Ralative to Root			Sheath/Blade		
Root			192.6	±	22.4	3559	±	578	262.6	±	34.3	1.35	$\times 10^4$	1					
Shoot			533.0	±	39.5	479	±	80	8.1	±	0.9	5.86	$\times 10^4$	4.28	±	0.51			
	L4	Blade	34.8	±	3.6	725	±	77	13.9	±	2.0	5.29	$\times 10^4$	3.89	±	0.31	1.49	±	0.32
		Sheath	35.1	±	3.9	478	±	84	6.3	±	1.2	7.98	$\times 10^4$	5.79	±	1.32			
	L5	Blade	65.0	±	4.6	642	±	154	10.7	±	1.1	6.05	$\times 10^4$	4.41	±	0.68	1.23	±	0.18
		Sheath	70.6	±	6.4	334	±	70	4.7	±	1.0	7.43	$\times 10^4$	5.42	±	1.05			
	L6	Blade	113.0	±	6.8	603	±	105	11.0	±	1.3	5.52	$\times 10^4$	4.04	±	0.46	1.23	±	0.17
		Sheath	94.6	±	15.6	297	±	69	4.4	±	0.6	6.84	$\times 10^4$	4.98	±	1.08			
	L7		43.3	±	17.8	111	±	37	2.4	±	1.0	5.00	$\times 10^4$	3.72	±	1.72			
	Others		76.4	±	2.3	612	±	105	12.2	±	2.4	5.12	$\times 10^4$	3.76	±	0.45			
Solution						0.274 mM			0.1μM			2.75	$\times 10^3$						

Figures

Fig. 1 Evaluation of the "simple subtraction" method using a NaI (Tl) scintillation counter to determine the potassium radionuclide $^{42}K^+$ amount in the test solution, with or without the cesium radionuclide $^{137}Cs^+$, which would support the use of a $^{42}K^+$–$^{137}Cs^+$ double-tracer experiment in the physiological study. (A) The decay mode of $^{42}K^+$ and $^{137}Cs^+$. (B) The gamma-ray spectrum emitted from one of the test solutions, which contained 640 Bq of $^{42}K^+$ and 80 Bq of $^{137}Cs^+$ at day 0. After 7 days, the $^{42}K^+$ peak (1,525 keV) disappeared from the spectrum and only $^{137}Cs^+$ peak (661.7 keV) was detected by the germanium (Ge) detector. (C) Relationship between the $^{42}K^+$ amount (cpm) derived from the simple subtraction method and the $^{42}K^+$ amount (Bq) determined by the Ge detector. The test solutions contained either 890 Bq of $^{137}Cs^+$ (black), 80 Bq of $^{137}Cs^+$ (gray), or 0 Bq of $^{137}Cs^+$ (white) in addition to $^{42}K^+$.

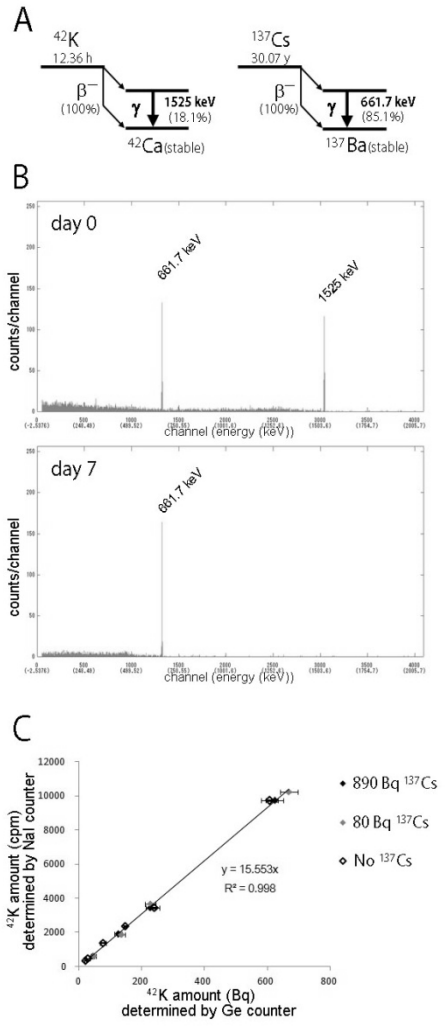

Fig. 2 Kinetic analysis of the potassium (K^+) concentration dependency of K^+ and cesium (Cs^+) uptake in the roots of 2-week-old rice plants grown in a full-nutrient solution containing 270 μM K^+ and 0.1 μM Cs^+.

Uptake was performed for 20 min in the nutrient solution with a varied K^+ concentration and a fixed 0.1 μM concentration of Cs^+, and radionuclides $^{42}K^+$ and $^{137}Cs^+$ were added simultaneously. (A) Uptake rate of K^+ (black spots) and Cs^+ (white triangles). (B) $^{42}K^+/^{137}Cs^+$ selectivity factor versus K^+ concentration in the medium. All values are means ± SD (n = 3−6).

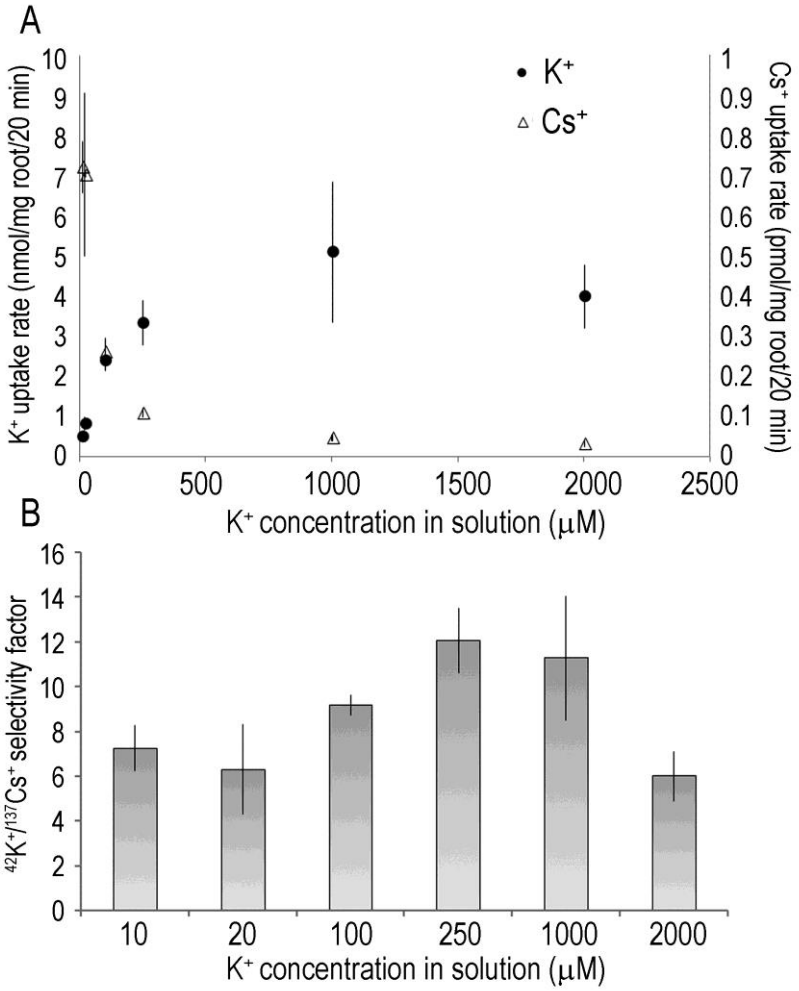

Fig. 3 Kinetics of the potassium (K^+) and cesium (Cs^+) translocation from rice roots to shoots analyzed by a real-time imaging system (RRIS).

(A) Four rice plants were placed on a plate scintillator. Then, the two left seedlings (K1 and K2) were treated with the potassium radionuclide $^{42}K^+$, while the two right seedlings (Cs1 and Cs2) received the radionuclide $^{137}Cs^+$. The roots were pressed on the scintillator using a blue polyurethane sheet. (B) The picture of the radionuclides taken using the RRIS at 4 h, when the solution in the root chamber was replaced with a solution without radionuclides, and the one captured at 8 h, when the sequential imaging had finished. The red boxes indicate the regions of interest (ROI) in which the signal intensity was determined. (C and D) Variations in the radionuclide amounts in the leaf ROI (C) and root ROI (D) over time. The normalized values relative to those at 4 h are shown. In (C), the lines obtained by the linear approximation ($R^2 > 0.99$) of $^{42}K^+$ (gray) and $^{137}Cs^+$ (black) signals between 3 and 5 h are presented**.** The experiment was carried out four times. and similar results were obtained.

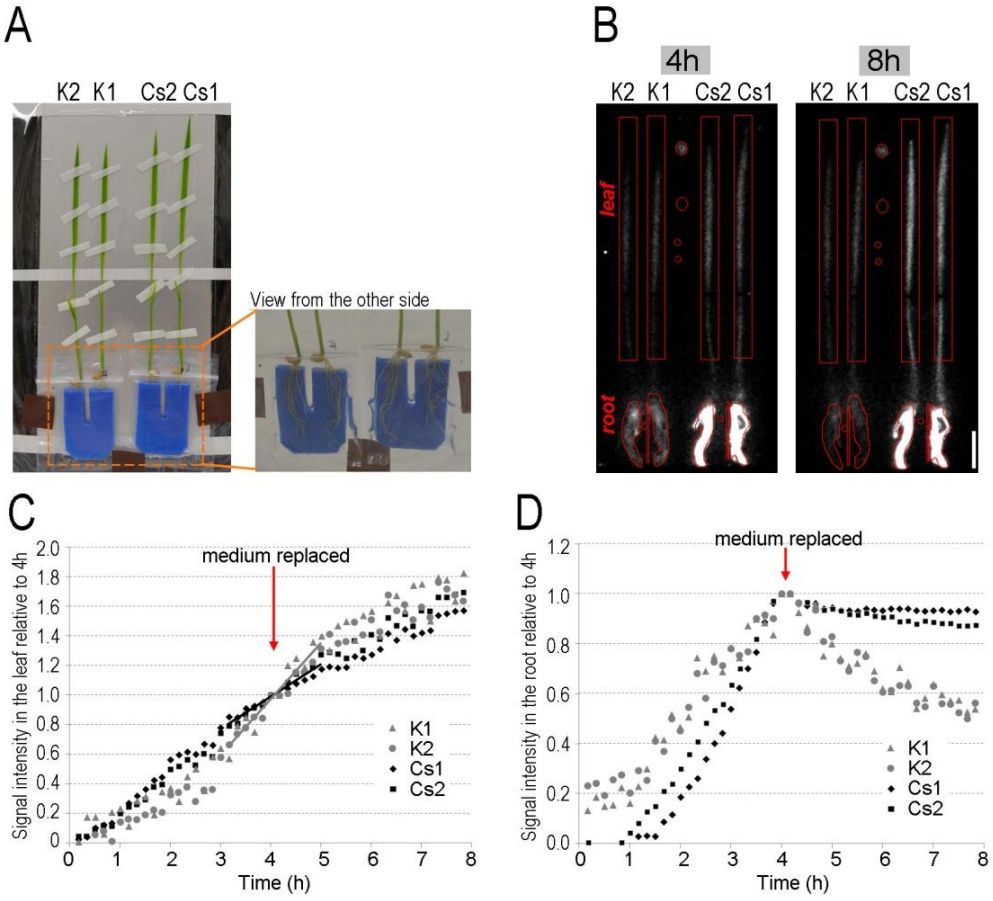

Fig. 4 Translocation of the potassium and cesium radionuclides $^{42}K^{+}$ and $^{137}Cs^{+}$, respectively, absorbed for one hour by a segment of the rice roots.
(A) The amount of radionuclides remaining in the radionuclide-added segment is presented as the percentage of the uptake amount. Values are means ± SD (n = 4). (B) The percentage distribution of the total radionuclides exported from the radionuclide-added segment into the shoots (black), the crown roots (light gray), the upper roots (white), and the bottom roots (dark gray).